Journal of Food Measurement and Characterization (2024) 18:7019–7028
https://doi.org/10.1007/s11694-024-02711-7

ORIGINAL PAPER

Extraction and electrochemical sensing of anthocyanins in berry fruits by use of carbon nanotube-based electrode

Liu Yang[1] · Sheng Chen[1] · Lingxi Zhao[2] · WenWen Chen[1] · Weifeng Huang[3] · Xiaona Li[3] · Hongyuan Zhang[2]

Received: 4 January 2024 / Accepted: 17 June 2024 / Published online: 1 July 2024

Abstract

This study uses a modified electrode made of Molecularly Imprinted Polymers (MIPs) and Multi-Walled Carbon Nanotubes (MWCNTs) to provide a unique method for the extraction and electrochemical detection of cyanidin in berry fruits. The special pairing of MIPs with MWCNTs improves the sensors' sensitivity and selectivity, allowing for accurate cyanidin detection and quantification. The electropolymerization procedure was used to create the electrode, and TEM, XRD, and Raman studies were used to confirm its structure. Using Differential Pulse Voltammetry (DPV), the electrochemical response of the MIP/MWCNTs/GCE sensor was investigated. With a detection limit of 0.14 mg/mL, the sensor showed a linear range of 0.5 mg/mL to 242 mg/mL, demonstrating good sensitivity and adaptability. Real samples (berry fruits, human urine, and tap water) were used to further validate the sensor's performance, and the results revealed a strong correlation with the UPLC technique. The DPV approach showed excellent accuracy and suitability with low relative standard deviation values (less than 4.66%) and adequate recovery values (97.00–99.50%). Excellent selectivity, repeatability, and stability characterize the suggested MIP/MWCNTs/GCE sensor, which makes it a viable instrument for real-world uses in the food and environmental industries. This work advances the field by offering a more selective and sensitive way to identify cyanidin in berry fruits.

Keywords Anthocyanins · Berry fruits · Cyanidin · Electrochemical sensing · Molecularly imprinted polymers · Multi-walled carbon nanotubes

Introduction

Anthocyanins are a class of naturally occurring pigments that are commonly found in plants, especially in fruits like berries, and they are members of the flavonoid group [1]. These substances are well known for their vivid red, purple, or blue hues, which improve the aesthetic appeal of numerous fruits. Beyond their aesthetic appeal, anthocyanins have attracted a lot of interest because of their possible health advantages, which include anti-inflammatory and antioxidant capabilities [2]. An increasing amount of research is being done on the electrochemical detection and analysis of anthocyanins in different fruits, such as berries, in an effort to determine their quantities and potential effects on human health. The emphasis on anthocyanin analysis is a reflection of the growing understanding of these compounds' importance to food science, nutrition, and public health as well as its function in enhancing well-being.

One particular kind of anthocyanin that is common in many fruits is called cyanidin, and it plays a significant role in the vivid colors of berries [3, 4]. Furthermore, cyanidin is an important antioxidant anthocyanin, which adds to its significance in the fields of nutrition and food research [5]. Fruit cyanidin identification and extraction are important processes that are necessary to comprehend the nutritional value and composition of fruits as well as to investigate any potential health benefits that may arise from their existence. Research on food quality, nutrition, and public health is being enhanced by the increased interest in cyanidin extraction, sensing, and analysis. These efforts are in line with the

✉ Hongyuan Zhang
zhanghy6970@sina.com

[1] College of Food Science and Engineering, Changchun University, Changchun 130022, China

[2] College of Chemistry, Baicheng Nomal University, Baicheng 137000, China

[3] Baicheng Shenbang Food and Agricultural Products Inspection and Testing Co, Baicheng 137000, China

larger endeavor to determine cyanidin content and possible effects on human health [6].

Numerous methodologies, including more sophisticated ones like chromatography and spectrophotometry [7, 8], as well as conventional ones like electrochemical methods [9], have been investigated in scientific investigations for the identification of anthocyanins. These techniques have clear benefits in terms of cost-effectiveness, speed, and sensitivity [10]. Furthermore, it has been apparent that using nanostructures in electrochemical sensors is a viable way to improve the accuracy and effectiveness of anthocyanin detection [11, 12]. These developments highlight the possibility for a more thorough comprehension of fruit anthocyanins and their effects on human health [13, 14].

Enhancing the performance and precision of electrochemical sensors requires the incorporation of nanostructures. These nanostructures have unique properties such as longer-lasting electrodes, faster electron transfer rates, increased selectivity, and increased sensitivity in electrochemical detection systems. Analyte detection is made much more reliable and efficient overall when sensors with nanostructures are integrated. These developments not only contribute to our growing understanding of fruit anthocyanins and their effects on human health, but they also broaden the range of potential uses for electrochemical sensors in a variety of contexts, including the assessment of food safety, environmental monitoring, and medical diagnostics [15].

When integrated into electrochemical sensors, molecularly-imprinted polymers (MIPs) and multi-walled carbon nanotubes (MWCNTs) have been coupled to generate nanocomposites, which have shown outstanding characteristics [16–18]. The resultant nanocomposites in electrochemical sensing systems show increased electrode durability, faster electron transfer rates, higher selectivity, and increased sensitivity [17, 19, 20]. With their ability to recognize molecules, MIPs provide targeted molecules with particular binding sites [21], and MWCNTs improve signal transduction and sensor performance [22], by increasing surface area and electrical conductivity. The distinct interaction between MIPs and MWCNTs in these nanocomposites efficiently increases the sensitivity and selectivity of electrochemical sensors, establishing them as potential instruments for accurate analyte detection and quantification in a range of applications, including food safety evaluation, environmental monitoring, and biomedical diagnostics [17, 19, 23].

An electrochemical sensor for the sensitive and selective detection of diuron in river water samples was created by Wong et al. [24] using a combination of carboxyl-functionalized multi-walled carbon nanotubes and a molecularly imprinted polymer. Ali et al. [25] demonstrated an electrochemical sensor based on a molecularly imprinted polymer for highly sensitive and selective detection of ceftizoxime. The MIP was synthesized via electropolymerization of poly-cysteine (on a multi-walled carbon nanotube modified glassy carbon electrode. A new electrochemical sensor for the detection of chloramphenicol was presented by Yang et al. [26]. To provide a dependable platform for chloramphenicol detection, the sensor made use of mesoporous carbon, three-dimensional porous graphene, and multi-walled carbon nanotubes@molecularly imprinted polymer. Together, these investigations advance our knowledge of how MIPs and MWCNTs work synergistically to improve sensor performance for a range of applications. To achieve optimal performance in electrochemical sensor design, material selection is crucial. The rationale for the specific material selection of MIPs and MWCNTs in the proposed cyanidin detecting sensor is sound. MIPs are artificial polymers that have particular binding sites intended to identify target molecules. Because of their specific binding affinity, they provide excellent selectivity. MIPs improve the sensor's specificity in cyanidin detection. MWCNTs also offer a wide surface area, which improves the adsorption of analytes. Efficient electron transmission is facilitated by their exceptional electrical conductivity. Sensor sensitivity is increased by electrodes treated with MWCNT. The suggested nanocomposite electrode's improved sensitivity and selectivity are a result of the complementary actions of MIPs and MWCNTs, which make it a viable method for precise cyanidin detection in berry fruits.

The goal of the project is to extract cyanidin from berry fruits and detect it electrochemically using an electrode modified with MIPs and MWCNT nanocomposite. This study is interesting because it aims to improve the sensitivity and selectivity of electrochemical sensors for the accurate identification and quantification of cyanidin by investigating the synergistic effects of MIPs and MWCNTs.

Experiments

Chemical

Ethanol (99.8%) and methanol (99%) were used in the extraction process. Hydrochloric acid (HCL, 37%) was purchased from Sigma-Aldrich in the United States. Alumina slurry (99%, 0.3–0.05 μm), glassy carbon electrode (GCE, 3 mm diameter), phosphate-buffered saline (PBS), multi-walled carbon nanotubes (MWCNTs, > 95%), and cyanidin chloride (≥ 95%) were acquired from Sigma-Aldrich, USA, for the electrode production process. Merck, Germany provided the following chemicals: nitric acid (HNO_3, 60%), sulfuric acid (H_2SO_4, 97%), dimethylformamide (DMF, 99%), L-cysteine (l-Cys, 99%), and sodium hydroxide

(NaOH, 98%). A double distillation of water was used to prepare each solution.

Instrumentation

Using a SilentCrusher M homogenizer from Heidolph, Germany, the berries were homogenized in an extraction solvent. A USA-sourced Allegra X-15R centrifuge from Beckman Coulter Inc. was used for the centrifugation procedure. A rotary evaporator from Buchi, Switzerland was used to evaporate the solvent. The extracts were analyzed using a Waters Corporation, USA Ultra Performance Liquid Chromatography (UPLC) system, and the total anthocyanins were quantified using an Agilent Technologies, USA UV/Vis detector.

A CS310 Electrochemical Workstation (Corrtest Instruments Co., Ltd., Wuhan, China) was used for the voltammetric tests. The working, reference, and auxiliary electrodes of the system were variously modified GCE, silver/silver chloride (Ag/AgCl (3 M KCl)), and Pt mesh electrodes, respectively. The system was configured using a standard three-electrode setup. Using Differential Pulse Voltammetry (DPV), the electrochemical response of the MIP/MWCNTs/GCE sensor was examined in order to evaluate its efficacy in cyanidin detection. Key factors including the potential range and scan rate were changed to optimize the DPV tests. To guarantee the best sensitivity and resolution in identifying the target analyte, the ideal scan rate and possible range were ascertained. All ensuing DPV measurements were subsequently conducted using these optimized values. Tests using cyclic voltammetry were conducted at a scan rate of 50 mV/s. A pulse amplitude of 20 mV, a pulse width of 50 ms, and a step increase of 2 mV were used for the differential pulse voltammetry tests. The electrolyte in the electrochemical analyses was a 0.1 M PBS solution. A pH meter (pHS-3 C, Shanghai REX Instrument Factory, China) was used to measure and adjust the pH of the PBS solution until it reached 7.4. Four times the measurements were made, and the average results were given together with the relevant statistical analysis. The Bruker D8 DISCOVER (Bruker Corporation, with its headquarters located in Billerica, Massachusetts, USA) was utilized for X-ray diffraction (XRD) examination.

Preparation of the electrode

The GCE surface was meticulously polished using a microfiber cloth and alumina slurry. Following a 5-minute ultrasonication in ethanol, ultrapure water, and diluted nitric acid, it was washed with ultrapure water. Next, utilizing CV for 15 cycles at 50mV/s scan rate and within a potential range of -1 to 1 V, the GCE was treated with 1M H_2SO_4 in 0.1 M PBS. After that, the GCE surface was drop-casted with a 20 µL volume of a 1 mg/ml suspension of MWCNTs in DMF solution, and it was then allowed to dry at room temperature. The process of electropolymerization was used to create non-imprinted polymer (NIP) [27]. The NIP-modified electrode (NIP/MWCNTs/GCE) was prepared by immersing the MWCNTs/GCE in a solution of 0.1 M PBS (pH 5) that contained 200 µM of cyanidin and 1 mM of l-Cys. By subjecting the immersed MWCNTs/GCE surface to 15 min of CV at a potential range of -0.75 to 1.2 V, the surface was electropolymerized. The molecularly imprinted polymer-modified electrode was used to construct the MIP electrode. To extract the template molecule (cyanidin) from the imprinted polymeric layer, the electrode was submerged in 0.3 M of NaOH for eight minutes. The modified electrode that was produced is now known as MIP/MWCNTs/GCE.

Extraction and preparation real samples

During the experiment, freezing water was used to clean white mulberry that were purchased at a nearby market. Following cleaning, the berries were kept at -20 °C for a full day before being submerged in liquid nitrogen and kept at -80 °C until the extraction procedure was completed [28]. There were multiple steps in the extensive extraction procedure. The frozen berries were first allowed to defrost at room temperature. The berries were then blended in an extraction solvent using a Silent Crusher M homogenizer, or they were crushed using a mortar and pestle. After that, the berries were macerated for 48 h in methanol with 0.1% 12 N HCL. During the extraction process, the fruit pulp was once again mixed with fresh solvent while the original extraction solvent was kept. The extracts were mixed and centrifuged after 48 h. The solvent was evaporated, and the supernatant was kept. After being diluted and filtered, the leftover extract was kept at -20 °C until UPLC study. The thawed berry pieces were homogenized in the extraction solvent in a similar fashion to extract cyanidin. At 37 °C, the samples were extracted for ninety minutes. After the samples were extracted, they were centrifuged, and the supernatant was then poured into a flask with a circular bottom. A rotary evaporator was then used to evaporate the solvent. Before UPLC and electrochemical analysis, the residual extract was filtered, diluted, and kept at -20 °C.

Furthermore, the amount of cyanidin in the extract was determined using electrochemical tests. The standard addition procedure was used to determine the recovery value and cyanidin in genuine samples, and the extract solution was utilized to prepare 0.1 M PBS.

A healthy participant's urine sample was collected in order to prepare the human urine sample. For ten minutes, the sample was centrifuged at 4000 rpm in order to

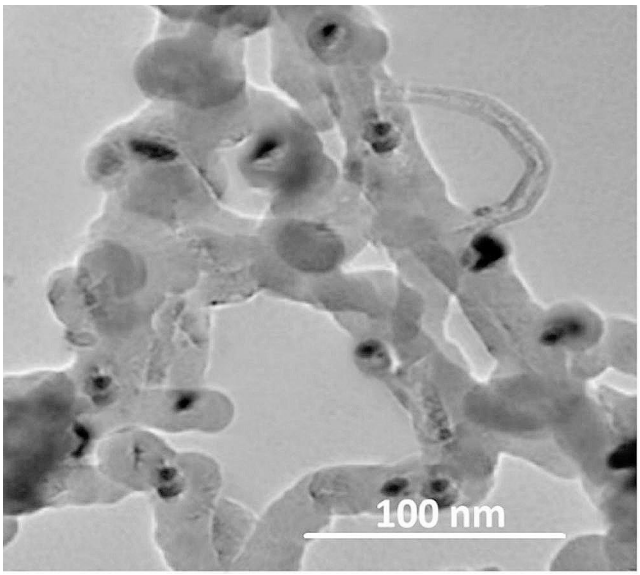

Fig. 1 TEM image of MIP/MWCNTs.

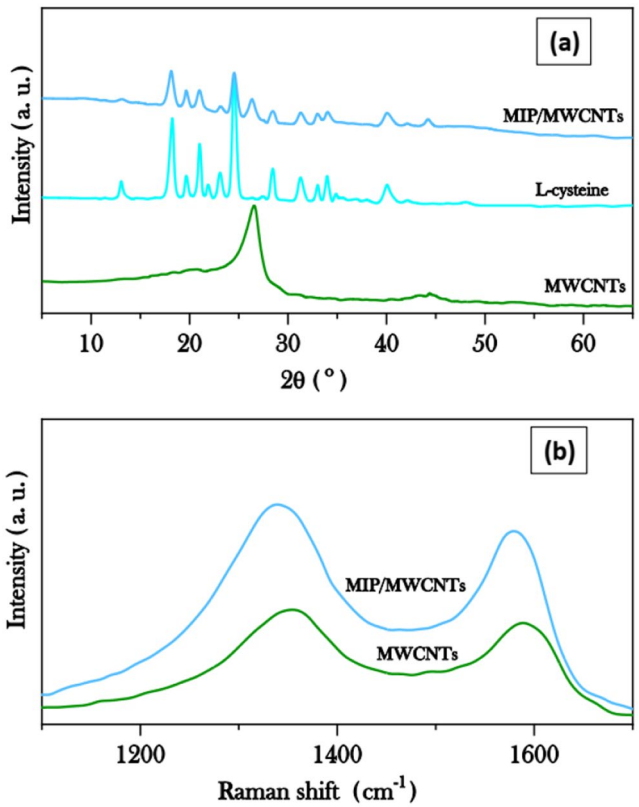

Fig. 2 (**a**) The XRD patterns for MWCNTs, L-cysteine, and MIP/MWCNTs, and (**b**) Raman spectra of MIP/MWCNTs and MWCNTs

eliminate any solid particles. The liquid part that was left over was then diluted ten times with 0.1 M PBS (pH 7.4) in order to prepare it for analysis. In order to utilize the tap water sample as a genuine sample for analysis, it was also utilized to prepare 0.1 M PBS (pH 7.4) rather than double distilling the water.

Results and discussion

Morphological and structural characterizations

The MIP/MWCNTs/GCE TEM picture was examined. Figure 1's TEM picture shows that the MIP and MWCNTs were successfully included. There seems to be a well-formed composite structure as the MIP is evenly distributed over the MWCNTs. The clear contrast between the MIP and MWCNTs in the high-resolution TEM image further verifies the existence of MIP on the MWCNTs. The GCE was successfully modified with MWCNTs and MIP, indicating that their combined benefits may enhance sensor performance.

Figure 2a shows the XRD patterns for MWCNTs, L-cysteine, and MIP/MWCNTs. Two unique diffraction peaks can be seen in the XRD pattern for MWCNTs: a prominent C (002) peak at approximately 26.51°, which is representative of the graphite peak, and a peak at approximately 43.88°, which is representative of the (100) planes of the nanotube structure. The XRD patterns for L-cysteine support the previously published XRD investigations of the compound [29–31] by displaying reflection lines that correspond with the monoclinic system (space group P21). A few L-cysteine peaks and MWCNT peaks can be seen in the XRD pattern of the MIP/MWCNTs composite, showing that L-cysteine was successfully electropolymerized on MWCNTs.

Figure 2b shows the Raman spectra of MIP/MWCNTs and MWCNTs. The MWCNTs spectrum shows two prominent peaks: the graphitic lattice (G) peak at 1593 cm^{-1}, which originates from the first order scattering of the E2 g phonon of the sp^2 carbon lattice [32], and the defect (D) peak at 1350 cm^{-1}, which is attributed to the breathing mode of k-point phonons with A1g symmetry [33, 34]. The D-band shifts from 1350 cm^{-1} to 1347 cm^{-1} while the G-band shifts from 1593 cm^{-1} to 1582 cm^{-1} for MIP/MWCNTs. The functionalization of organic molecules on the surfaces of the carbon layer is shown by these shifts in the D and G bands. This demonstrates that the L-cysteine molecules have been effectively functionalized on the MWCNT surface [35–37]. These findings validate that L-cysteine molecules are functionalized on the surface of the MWCNTs and are in line with other scientific data. The correctness of findings regarding MWCNTs is validated by this consistency with the body of current literature.

Using three complementing approaches, the morphological and structural characteristics of the MIP/MWCNTs electrode were thoroughly analyzed. The successful integration of MIP and MWCNTs into the composite is visually

confirmed by TEM. A well-formed composite structure was revealed by the uniform distribution of MIP across the MWCNTs. Moreover, crucial information about crystallography was disclosed by XRD patterns. The presence of MWCNTs was confirmed by the different peaks detected for them, namely the (100) planes of the nanotube structure and the C (002) peak, which represents the graphite lattice. Furthermore, L-cysteine's XRD patterns matched those found in the literature, indicating that it had a monoclinic system. Raman spectroscopy additionally shed light on molecular functionalization. The MIP/MWCNTs' D and G band shifts showed that L-cysteine molecules had been functionalized on the MWCNT surface. Together, these consistent results confirm the MIP/MWCNTs electrode's structural properties and highlight the electrode's potential for improved sensor performance.

Electrochemical characterization

The cyclic voltammograms of the electrodes GCE, MWCNTs/GCE, NIP/MWCNTs/GCE, and MIP/MWCNTs/GCE are shown in Fig. 1. The electrodes were tested at 50mV/s scan rate in 0.1 M PBS with and without 5 mg/mL cyanidin. Due to the MWCNTs' greater surface area and electrical conductivity, the MWCNTs/GCE displays a higher background current than the GCE [38]. Both the MIP/MWCNTs/GCE and the NIP/MWCNTs/GCE exhibit a l-Cys oxidation peak at around + 0.50 V. However, the MIP/MWCNTs/GCE shows a bigger peak current and a lower peak potential for l-Cys oxidation, which can be explained by the improved electrocatalytic activity of the MIP layer [39]. An oxidation peak is seen for MWCNTs/GCE, NIP/MWCNTs/GCE, and MIP/MWCNTs/GCE when cyanidin is added. The MIP/MWCNTs/GCE exhibits the largest peak current because of the cyanidin's preferential binding in the imprinted cavities of the MIP layer [40–42]. This demonstrates how the MIP layer improves the electrode's electrochemical performance and how MIP/MWCNTs/GCE could be a viable platform for the sensitive detection of cyanidin. The MIP layer is absent from the NIP/MWCNTs/GCE, in contrast, which reduces its sensitivity and selectivity towards the target molecule. MIP/MWCNTs/GCE is a potent instrument for the selective detection of target molecules because of its novel detection mechanism, which combines molecular imprinting for selectivity and electrochemical detection for sensitivity. As a result, the electrochemical analysis of MIP/MWCNTs/GCE was carried out Fig 3.

Optimization the sensor's performance

The impact of pH on the sensor's response and the influence of electropolymerization duration on electrode fabrication were considered in order to maximize the sensor's performance. The CV response of MIP/MWCNTs/GCE in a 0.1 M PBS containing 5 mg/mL cyanidin was investigated at different pH levels in order to investigate the impact of pH on sensor response. The sensor responds to the analyte by displaying the largest peak current (Fig. 4a). This indicates

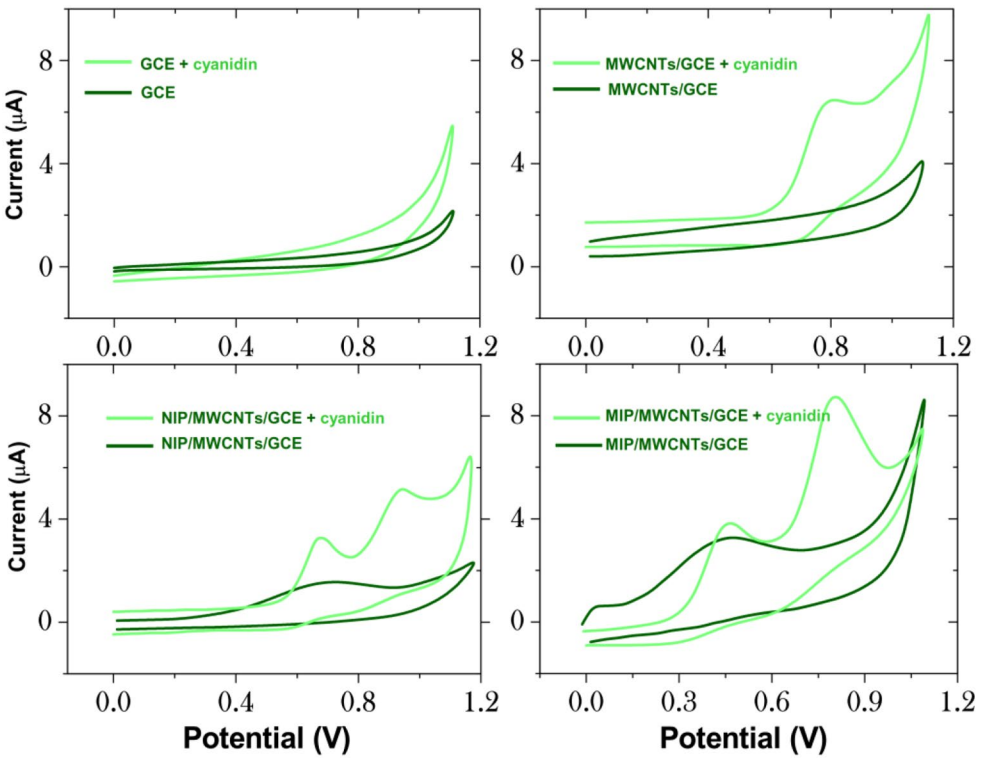

Fig. 3 The cyclic voltammograms of GCE, MWCNTs/GCE, NIP/MWCNTs/GCE, and MIP/MWCNTs/GCE, in a 0.1 M PBS environment, with and without 5 mg/mL cyanidin

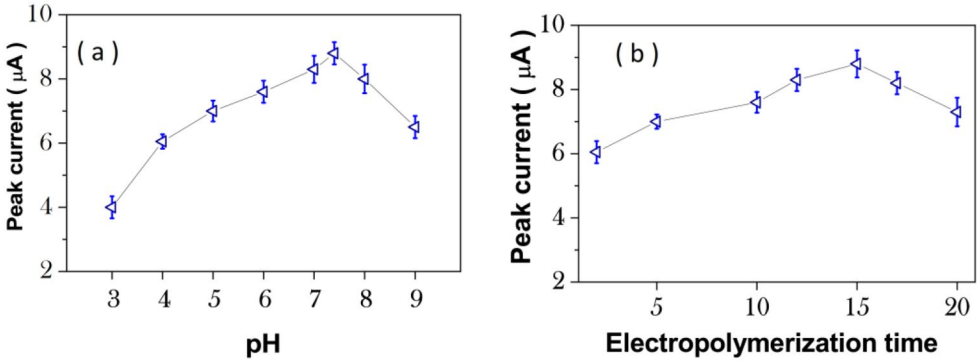

Fig. 4 (**a**) Study the effect of pH on sensor response and (**b**) effect of electropolymerization time on the construction of the electrode the CV response of MIP/MWCNTs/GCE, in a 0.1 M PBS containing 5 mg/mL cyanidin

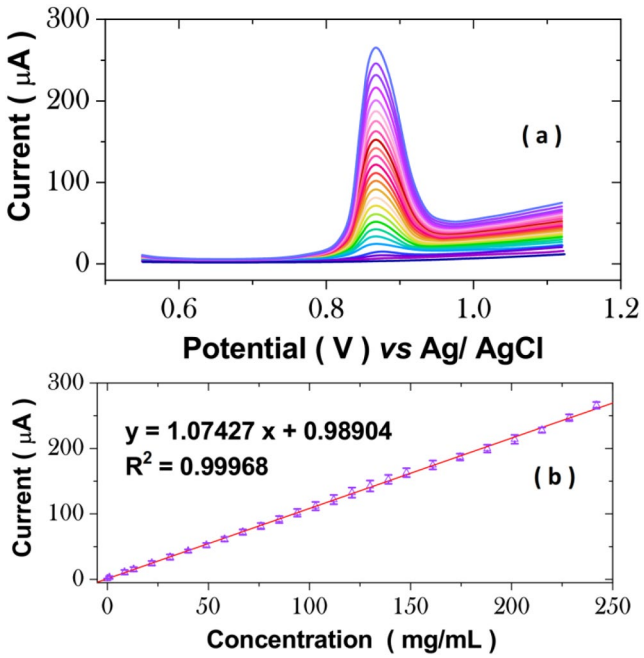

Fig. 5 obtained DPV using a MIP/MWCNTs/GCE in a 0.1 M PBS electrolyte, across various concentrations of cyanidin and the analytical plot of the anodic peak current vs. cyanidin concentrations

that the ideal conditions for the electrochemical processes involved in the detection process are found. That's why this pH was used for all later research.

The impact of the electropolymerization time on the electrode construction was also investigated in order to optimize the electrode building time. In reaction to the analyte in the electrochemical cell, Fig. 4b demonstrates that the maximum peak current was obtained after a 15-minute accumulation time. This implies that within an accumulation time of fifteen minutes, the ideal formation of the imprinted polymeric coating on the electrode surface can occur. As a result, this period of time was thought to be the best accumulation window for electrode building. These two investigations shed important light on the characteristics influencing the MIP/MWCNTs/GCE sensor's performance and emphasize how crucial it is to optimize these parameters in order to detect the target analyte with accuracy and dependability.

Table 1 Sensing performance of designed cyanidin sensor in current study and other reported cyanidin sensor in literatures

Method	LOD (mg/mL)	Linear range (mg/mL)	Ref.
DPV	0.14	0.5 to 242	This work
UHPLC-MWD-UHR-Q-TOF-MS	3.68	5 to 200	[45]
LC-MS	1	1 to100	[46]
HPLC-DAD	4.8	----	[47]
HPLC/UV	1.5×10^{-4}	1.25×10^{-4} to 0.2	[50]

Electrochemical response study of MIP/MWCNTs/GCE

Using a MIP/MWCNTs/GCE in a 0.1 M PBS electrolyte, DPV was used to detect cyanidin at different concentrations. This technique was selected because it can accurately and sensitively detect variations in current as a function of applied voltage [43, 44]. The obtained DPV and the analytical plot of cyanidin's anodic peak current against its various concentrations are shown in Fig. 5a and b. It is clear that when analyte concentrations grow, the anodic current increases. This is a common behaviour seen in electrochemical sensors, where the analyte's concentration is proportionate to the current response. The cyanidin calibration curve displays a linear range of 0.5 mg/mL to 242 mg/mL ($R^2=0.99968$) with a 0.14 mg/mL technique detection limit ($S/N=3$). The LOD was calculated using the formula $LOD=3\ \sigma/s$, where σ represents the standard deviation of the five blank measurements, and s denotes the slope from the calibration curve. This broad linear range and low detection limit point to the suggested sensor's great sensitivity and adaptability. Table 1 presents a comparison of the current results with other earlier publications for the electrochemical detection of cyanidin. The proposed sensor appears to be more sensitive than UHPLC-MWD-UHR-Q-TOF-MS, LC-MS, and HPLC-DAD, it can be concluded [45–47]. The distinct characteristics of the MIP/MWCNTs/GCE, such as the MIP layer's selective recognition of the target molecule

and the MWCNTs' increased electrical conductivity, are responsible for this better performance [48, 49]. The sensing performance of the proposed cyanidin sensor used in this investigation is compared with other cyanidin sensors that have been published in the literature in Table 1. This comparison is essential for assessing the suggested sensor's performance in relation to current techniques and pinpointing areas in need of further development.

The combination of MIPs with MWCNTs results in improved sensitivity and selectivity, which is explained by the synergistic interaction of their unique features. The MIP layer forms complementary cavities during the polymerization process, giving the target analyte (cyanidin) extremely selective recognition sites. By ensuring that only the target molecule is bound, this selective binding reduces interference from other substances in the sample. Meanwhile, the MWCNTs improve overall sensor performance by offering a large surface area that facilitates effective electron transfer pathways and enhanced analyte capture. Rapid electron transit made possible by the MWCNTs' exceptional electrical conductivity produces a brighter and more pronounced signal during electrochemical detection. The sensor's sensitivity and selectivity have been greatly increased as a result of the excellent electron transport provided by MWCNTs and the selective analyte binding of the MIP layer.

The sensing capabilities of our recently suggested cyanidin sensor and a few previously published sensors from the literature are compiled in Table 1. Our method has a better detection limit of 0.14 mg/mL than UHPLC-MWD-UHR-Q-TOF-MS at 3.68 mg/mL, LC-MS at 1 mg/mL, HPLC-DAD at no given value, and HPLC/UV at 1.5×10^{-4} mg/mL, which has a lower detection limit but a narrower linear range from 1.25×10^{-4} mg/mL to 0.2 mg/mL, as the table illustrates. In addition, our sensor has a linear dynamic range that is wider than the limited ranges observed in the traditional methods, ranging from 0.5 mg/mL to 242 mg/mL. These improvements result in increased cyanidin level analysis precision, accuracy, and applicability across a range of sample matrices. Our work thus lays the groundwork for novel developments in the creation of reliable and effective sensors utilising MIPs and MWCNTs, creating chances to meet a wide range of analytical needs in many chemical domains.

The results of this investigation mark a significant breakthrough in the creation of electrochemical sensors for cyanidin detection and measurement. The suggested MIP/MWCNTs/GCE sensor outperforms conventional methods such as UHPLC-MWD-UHR-Q-TOF-MS, LC-MS, and HPLC-DAD in terms of sensing performance throughout a wide linear dynamic range and low detection limit. The synergistic actions of MIPs and MWCNTs are responsible for this accomplishment. We guarantee selective cyanidin adsorption while reducing nonspecific interactions by utilising MIPs' capacity to construct specialised recognition sites, greatly enhancing the selectivity of the sensor. Additionally, MWCNTs improve detectability by magnifying signal intensities for better detection thanks to their wide surface areas and efficient electron transport channels. Overall, this study highlights the enormous potential of incorporating MIPs and MWCNTs into sensor designs, providing viable ways to broaden the range of potential uses beyond cyanidin detection and making a significant contribution to the advancement of engineering and scientific knowledge in the domains of electrochemical and biosensors.

Reproducibility, and stability of the modified electrode

Three main criteria were used to assess the MIP/MWCNTs/GCE sensor's performance: selectivity, stability, and reproducibility. When evaluating the overall effectiveness and dependability of the sensor, these factors are crucial. As seen in Fig. 6a, reproducibility was evaluated by doing multiple DPV measurements with the same electrode. The findings showed a steady current response with less than 2% variation for various analyte sample concentrations, demonstrating the sensor's dependable operation at various analyte concentrations. This consistency is essential for reproducibility since it guarantees that the sensor can produce accurate readings under the same circumstances.

Another important factor, stability, was assessed by tracking the weekly DPV curve of 5 mg/mL of cyanidin after the sensor was preserved at 4°C in a refrigerator. After three weeks of preservation, the peak response showed no deviation, as revealed in Fig. 6b. This implies that, crucial to stability, the sensor continues to function over time—even during refrigerated storage. A stable sensor is appropriate for real-world applications because it consistently produces accurate and dependable readings. The reproducibility of the sensor construction method was assessed using four MIP/MWCNTs/GCEs that were prepared independently. Figure 6c shows that these electrodes had a relative standard deviation (RSD) of approximately 3.79% for cyanidin sensing at a concentration of 5 mg/mL. This attests to the sensor production method' high degree of consistency. The goal of this particular study was to conduct electrochemical testing to assess the selectivity, stability, and reproducibility of the MIP/MWCNTs/GCE sensor. Our main goal was to evaluate the sensor's dependability and performance in cyanidin detection under varied circumstances. The main objective of the data analysis was to evaluate the sensor's stability, repeatability, and consistency of response over time and in various storage scenarios. Through various measurements, preservation tests, and fabrication repeatability evaluations,

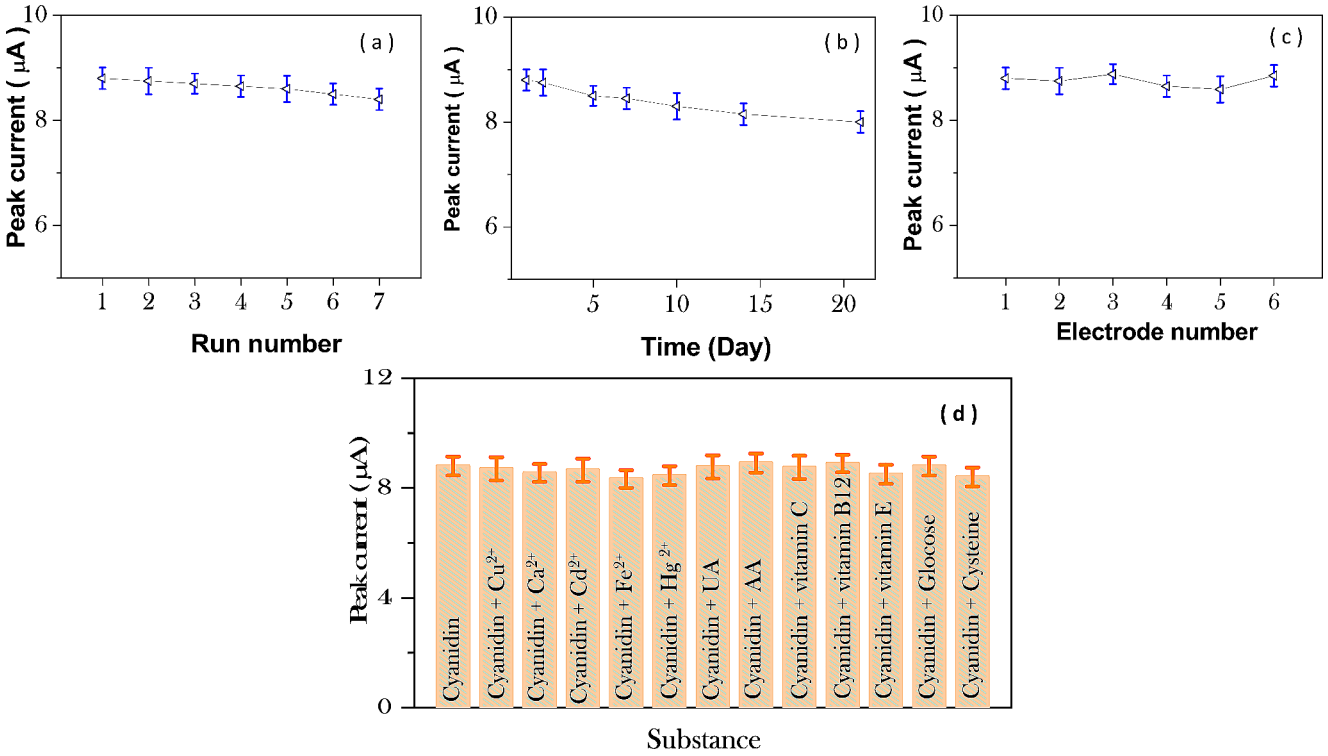

Fig. 6 Evaluation of the MIP/MWCNTs/GCE sensor's performance using DPV measurements for oxidation cyanidin in 0.1 M PBS containing 5 mg/mL cyanidin solution, (**a**) repeatability assessment a series of repetitive DPV measurements using the same electrode (**b**) Stability evaluation of peak response after three weeks of preservation at 4 °C, (**c**) Reproducibility assessment a series of repetitive DPV measurements using the six prepared electrodes under the same condition and (**d**) selectivity in present 10-fold concentrations various compounds and metal ions

the sensor's performance is thought to have been demonstrated, offering a thorough overview of its usefulness in real-world applications.

The improved electrode's selectivity was tested against a range of chemicals and metal ions, such as uric acid (UA), ascorbic acid (AA), glucose, cysteine, vitamin C, vitamin B12, vitamin E, Cu^{2+}, Ca^{2+}, Cd^{2+}, Fe^{2+}, Hg^{2} at 10-fold concentrations. The findings presented in Fig. 6d demonstrate that the cyanidin oxidation signals show stability when exposed to all interfering compounds (< 5.6%). This suggests that the sensor's selectivity is confirmed by its capacity to differentiate the target analyte from these other substances. In order to minimize the possibility of false positives, high selectivity is crucial to sensor performance as it guarantees that the sensor can reliably detect the target analyte even in the presence of other chemicals. As a result, the suggested MIP/MWCNTs/GCE sensor displays great stability, selectivity, and repeatability in cyanidin detection, making it a useful instrument for real-world uses. These qualities are essential to a sensor's functioning because they ensure reliable and accurate results throughout time and in a variety of testing conditions. As a result, the sensor becomes an invaluable instrument for identifying certain target molecules in a range of applications.

Real sample analyses

Real samples that had been prepared were used to confirm and validate the suggested sensing method's accuracy. In a 0.1 M PBS electrolyte solution made from these actual samples, Table 2 displays the outcomes of the UPLC method as well as the electrocatalytic peak current obtained from DPV measurements. For both the DPV and UPLC procedures, analytical studies were carried out using the conventional addition method; the outcomes are shown in Table 2. These findings demonstrated a strong link between the two techniques. Additionally, the DPV method demonstrated its great precision and adaptability with satisfactory recovery values (97.00–99.50%) and low relative standard deviation values (less than 4.66%). This demonstrates that the use of MIP/MWCNTs/GCE for deterrence in the food and environmental sectors is valid. Using actual berry fruit samples, the accuracy and precision of the MIP/MWCNTs/GCE sensor's performance was compared with that of the UPLC approach. Table 2 displays that the DPV method had low relative standard deviation values and good recovery values, demonstrating a strong connection with UPLC results. This implies that for the analysis of cyanidin in actual samples, the MIP/MWCNTs/GCE sensor provides accuracy and

Table 2 The resulted electrocatalytic peak current of DPV measurements and UPLC. ($n=4$)

Sample	Spiked (mg/mL)	DPV			UPLC		
		Detected (mg/mL)	Recovery (%)	RSD (%)	Detected (mg/mL)	Recovery (%)	RSD (%)
berries	0.0	211.2	---	4.66	209.0	---	4.12
	10.0	220.9	97.00	4.25	218.9	99.00	3.32
	15.0	225.9	98.00	4.03	223.9	99.33	4.59
	20.0	230.9	98.50	4.12	228.6	98.00	3.37
Tap water	0.0	0.0	---	4.21	0.0	---	4.41
	10.0	9.9	99.00	4.04	10.1	101.00	3.85
	15.0	14.8	98.66	3.78	14.9	99.33	3.69
	20.0	19.9	99.50	4.20	19.9	99.50	3.67
Human Urine	0.0	0.0	---	4.61	0.0	---	3.52
	10.0	9.9	99.00	3.21	10.0	100.00	4.02
	15.0	14.9	99.33	3.53	14.9	99.33	2.89
	20.0	19.8	99.00	3.72	19.9	99.50	3.37

precision that are on par with the traditional UPLC method. Notably, for the purpose of determining the amount of cyanidin in berry fruits, the DPV method offered a simple and affordable substitute for UPLC.

Conclusion

This work has effectively illustrated a new method for cyanidin extraction and electrochemical fruit sensing. Utilizing a modified electrode made of Multi-Walled Carbon Nanotubes (MWCNTs) and Molecularly Imprinted Polymers (MIPs) has verified to be a major breakthrough in the sector. It has been demonstrated that the special combination of MIPs and MWCNTs improves the sensors' sensitivity and selectivity, allowing for accurate cyanidin identification and quantification. This opens up new possibilities for the focused detection of molecules in a range of applications, which is a significant development in the field of electrochemical sensors. The thorough extraction method this study devised and the application of cutting-edge analytical techniques have guaranteed the correctness and dependability of the findings. Using actual samples, the sensor's performance was further verified, and the results shown a strong association with the UPLC technique. The suggested MIP/MWCNTs/GCE sensor also shows good selectivity, repeatability, and stability, which makes it a viable tool for real-world uses in the food and environmental sectors. This work advances the field by offering a more selective and sensitive way to identify cyanidin in berry fruits. Finally, the results of this investigation have significant ramifications for the development of electrochemical sensing in the future. A major advancement in the field has been made with the effective use of MIPs and MWCNTs in the creation of a highly selective and sensitive sensor for cyanidin detection. This study opens up new avenues for the creation of electrochemical sensors, which could find use across a range of sectors. It is envisaged that this work will stimulate additional study in this field, resulting in the creation of ever more potent and sophisticated sensors. For cyanidin detection in practical situations, the suggested MIP/MWCNTs/GCE sensor presents a number of benefits, especially for the food and environmental sectors. Its great sensitivity and selectivity, together with its affordability and usability, make it a viable instrument for quick on-site investigation. By offering a portable, real-time cyanidin level monitoring system, this sensor surpasses conventional techniques and improves quality control in food production and environmental monitoring applications. It is an invaluable tool for ensuring food safety and determining environmental pollution because of its capacity for on-site examination and real-time feedback. Although it has limits, our investigation on cyanidin detection utilizing the MIP/MWCNTs nanocomposite electrode provides insightful information. First, the cyanidin content may be impacted by sample variability resulting from varying fruit varieties and growth environments. Second, it's important to take into account any possible influence from other substances in intricate matrices. Finally, it is imperative to look into the electrode's long-term stability. The practical value of the sensor will be improved in the future by verifying it in real-world applications, optimizing materials, and downsizing the design.

Acknowledgements This work was sponsored by Jilin Provincial Science and Technology DepartmentGrant/Award Number: 20220202082NC; Jilin Provincial Department of EducationGrant/Award Number: JJKH20230682KJ.

References

1. J. Martín, M.J. Navas, A.M. Jiménez-Moreno, A.G. Asuero, Phenolic compounds-natural Sources Importance Appl. **117** (2017)
2. J.M. Bueno, P. Sáez-Plaza, F. Ramos-Escudero, A.M. Jiménez, R. Fett, A.G. Asuero, Crit. Rev. Anal. Chem. **42**, 126 (2012)

3. T. Pervaiz, J. Songtao, F. Faghihi, M.S. Haider, J. Fang, J. Plant. Biochem. Physiol. **5**, 1 (2017)
4. N.A. Almujally, D. Khan, N. Al Mudawi, M. Alonazi, A. Alazeb, A. Algarni, A. Jalal, H. Liu, *Sensors* 24, (2024)
5. Â. Luís, A.P. Duarte, L. Pereira, F. Domingues, Eur. Food Res. Technol. **244**, 175 (2018)
6. Q. Liu, L. Liu, Y. Zheng, M. Li, B. Ding, X. Diao, H.-M. Cheng, Y. Tang, Natl. Sci. Rev. **11**, (2024)
7. C.T. da Costa, D. Horton, S.A. Margolis, J. Chromatogr. A **881**, 403 (2000)
8. J. Lee, C. Rennaker, R.E. Wrolstad, Food Chem. **110**, 782 (2008)
9. A.A. de Lima, E.M. Sussuchi, W.F. De Giovani, Croat. Chem. Acta. **80**, 29 (2007)
10. X. Lin, P.P. Liu, J. Yan, D. Luan, T. Sun, X. Bian, Anal. Chem. **95**, 5561 (2023)
11. J.N. Tiwari, V. Vij, K.C. Kemp, K.S. Kim, ACS nano. **10**, 46 (2016)
12. B. Bai, T. Xu, Q. Nie, P. Li, Int. J. Heat Mass Transf. **153**, (2020)
13. M.B. Mock, S. Zhang, K. Pakulski, C. Hutchison, M. Kapperman, T. Dreischarf, R.M. Summers, J. Biotechnol. **379**, (2024)
14. C. Zhang, A.P. Awasthi, J. Sung, P.H. Geubelle, N.R. Sottos, Int. J. Fract. **208**, (2017)
15. A. Hosseinian-Roudsari, S.-A. Shahidi, A. Ghorbani-HasanSaraei, S. Hosseini, F. Fazeli, Food Chem. Toxicol. **168**, (2022)
16. J. Zhang, X.-T. Guo, J.-P. Zhou, G.-Z. Liu, S.-Y. Zhang, Mater. Sci. Engineering: C **91**, 696 (2018)
17. D. Nie, Z. Han, Y. Yu, G. Shi, Sens. Actuators B **224**, 584 (2016)
18. W. Shi, C. Zhou, Y. Zhang, K. Li, X. Ren, H. Liu, X. Ye, Biomed. Signal Process. Control **85**, (2023)
19. Y. Ma, X.-L. Shen, Q. Zeng, H.-S. Wang, L.-S. Wang, Talanta. **164**, 121 (2017)
20. Y. Shen, H.-. Gu, L. Zhai, B. Wang, S. Qin, D.-. Zhang, Biochim. et Biophys. Acta (BBA)-Molecular Cell. Biology Lipids **1867**, (2022)
21. F. Cui, Z. Zhou, H.S. Zhou, Sensors. **20**, 996 (2020)
22. A. Saleh Ahammad, J.-J. Lee, M.A. Rahman, *sensors* 9, 2289 (2009)
23. T. Anirudhan, V. Athira, V.C. Sekhar, Polymer. **146**, 312 (2018)
24. A. Wong, M.V. Foguel, S. Khan, F.M. Oliveira, C.R.T. Tarley, M.D.P.T. Sotomayor, Electrochim. Acta. **182**, 122 (2015)
25. M.R. Ali, M.S. Bacchu, M.R. Al-Mamun, M.M. Rahman, M.S. Ahommed, M.A.S. Aly, M.Z.H. Khan, J. Mater. Sci. **56**, 12803 (2021)
26. G. Yang, F. Zhao, Biosens. Bioelectron. **64**, 416 (2015)
27. M. Ali, M. Bacchu, M. Al-Mamun, M. Rahman, M. Ahommed, M.A.S. Aly, M. Khan, J. Mater. Sci. **56**, 12803 (2021)
28. M.L. Blackhall, R. Berry, N.W. Davies, J.T. Walls, Food Chem. **256**, 280 (2018)
29. Y. Su, E.P. Hessou, E. Colombo, G. Belletti, A. Moussadik, I.T. Lucas, V. Frochot, M. Daudon, S. Rouzière, D. Bazin, Amino Acids. **54**, 1123 (2022)
30. J. Chen, B. Bai, Q. Du, Mater. Today Commun. **39**, (2024)
31. C. Zhang, A.P. Awasthi, P.H. Geubelle, M.E. Grady, N.R. Sottos, Appl. Surf. Sci. **397**, (2017)
32. S. Gupta, A. Henson, B. Evans, R. Meek, Water Desal Treat. **162**, 97 (2019)
33. B. Mohanty, P.K. Parida, C.A. Bhuyan, B.R. TN, K. Laxmi, H. Jena, D. Ponraju, Diam. Relat. Mater. **139**, 110336 (2023)
34. A. Alazeb, B.R. Chughtai, N. Al Mudawi, Y. Alqahtani, M. Alonazi, H. Aljuaid, A. Jalal, H. Liu, Front. Neurorobotics. **18**
35. M. Zhang, X. Zhang, K. Zhao, Y. Dong, W. Yang, J. Liu, D. Li, Spectrochim. Acta Part A Mol. Biomol. Spectrosc. **266**, 120458 (2022)
36. S. Muralikrishna, K. Sureshkumar, T.S. Varley, D.H. Nagaraju, T. Ramakrishnappa, Anal. Methods. **6**, 8698 (2014)
37. H. He, W. Zhang, S. Ye, S. Li, Z. Nie, Y. Zhang, M. Xiong, W.-T. Chen, G. Hu, Surf. Interfaces **48**, (2024)
38. B. Singh, D. Singh, R. Mathur, T. Dhami, Nanoscale Res. Lett. **3**, 444 (2008)
39. G.S. Geleta, Sens. Bio-Sensing Res. **100610** (2023)
40. D. Dechtrirat, K.J. Jetzschmann, W.F. Stöcklein, F.W. Scheller, N. Gajovic-Eichelmann, Adv. Funct. Mater. **22**, 5231 (2012)
41. Y. Shen, H.-M. Gu, S. Qin, D.-W. Zhang, J. Mol. Cell Biol. **14**, (2022)
42. H. He, S. Ye, W. Zhang, S. Li, Z. Nie, X. Xu, W. Li, A. Abdukayum, W.-T. Chen, G. Hu, Chem. Eng. J. **489**, (2024)
43. X. Chen, H. Wu, X. Tang, Z. Zhang, P. Li, Electroanalysis **35**, e202100223 (2023)
44. B. Bai, J. Chen, F. Bai, Q. Nie, X. Jia, Environ. Technol. Innov. **33**, (2024)
45. S. Stuppner, S. Mayr, A. Beganovic, K. Beć, J. Grabska, U. Aufschnaiter, M. Groeneveld, M. Rainer, T. Jakschitz, G.K. Bonn, C.W. Huck, *Sensors* 20, 4983 (2020)
46. Y.O.E. Majdoub, M. Diouri, P. Arena, A. Arigò, F. Cacciola, F. Rigano, P. Dugo, L. Mondello, Eur. Food Res. Technol. **245**, 2425 (2019)
47. P. Pelizzo, M. Stebel, N. Medic, P. Sist, A. Vanzo, A. Anesi, U. Vrhovsek, F. Tramer, S. Passamonti, Biomed. Pharmacother. **157**, 114044 (2023)
48. R. Gui, H. Guo, H. Jin, Nanoscale Adv. **1**, 3325 (2019)
49. M.B. Mock, S. Zhang, B. Pniak, N. Belt, M. Witherspoon, R.M. Summers, Biotechnol. Notes **2**, (2021)
50. R. Yu, Y. Liu, P. Brown, U. Huber, Methods High-Quality Safe Authentic Herb. Prod. **1**, 3 (2020)